AIAA 81-0091R

Sound Generated by Rotor Wakes Interacting with a Leaned Vane Stator

J.B.H.M. Schulten*
National Aerospace Laboratory NLR, Amsterdam, the Netherlands

An unsteady three-dimensional lifting surface theory to predict the sound field of a stator with leaned, i.e., nonradial, vanes in an annular duct is presented. The duct carries a uniform subsonic main flow and is assumed to be anechoic. The sound is generated by the interaction of velocity disturbances with the stator vanes. The problem is formulated as an integral equation for the pressure jump across the vanes. This equation is solved by a Fourier series expansion, followed by a collocation procedure. The effect of vane lean on the sound field of a typical stator exposed to the viscous wake system of a rotor is studied. The modal distribution proves to be very sensitive to lean variation. Unless the rotor speed is very low (one mode cut-on), no reduction in the acoustic power at the blade passing frequency is found for any lean angle. On the contrary, even a moderate amount of lean raises the power significantly.

Nomenclature

$A_{n\mu}$ = modal pressure amplitude
c = rotor chord
c_d = rotor blade drag coefficient
$\boldsymbol{F}$ = force field
$FD_{n\mu}$ = function defined in Appendix A
$f_{n\mu}$ = function defined in Appendix A
(f_x, f_r, f_θ) = point force
G = Green's function
$g_{n\mu}$ = function defined in Appendix A
h = hub/tip ratio
$h_{n\mu}$ = function defined in Appendix A
$\boldsymbol{i}_x, \boldsymbol{i}_r, \boldsymbol{i}_\theta$ = unit vectors in cylindrical coordinate system
J = number of spanwise loading functions
j,k,l,n = summation integers
M = main flow Mach number
m = $k - nN$
N = number of vanes
$P_{kj\lambda}$ = pressure coefficient
p = pressure
Δp_j = pressure jump across jth vane
Δp_{kj} = pressure jump across jth vane caused by kth disturbance velocity component
q = tangential coordinate in rotor-fixed system, normal to s
r = radial coordinate
s = streamwise coordinate in rotor-fixed system
t = time coordinate
$U_{n\mu}(r), U'_{n\mu}(r)$ = radial eigenfunction, its derivative
V = number of wakes
$V_{n\mu}$ = function defined in Appendix A
$\boldsymbol{v}$ = velocity induced by the stator
v_n = component of $\boldsymbol{v}$ normal to the vanes
$W, W_{n\mu}$ = pure tone total, modal sound power
$\boldsymbol{w}$ = disturbance velocity
w_c = wake center velocity magnitude in rotor-fixed system
w_e = undisturbed velocity magnitude in rotor-fixed system
w_n = $\boldsymbol{w}$ component normal to the vanes
x, x' = axial coordinates
Y = wake width
β = $\sqrt{1-M^2}$
$\beta_{n\mu}$ = $\omega\sqrt{1-(\epsilon_{n\mu}\beta/\omega)^2}$ if $(\epsilon_{n\mu}\beta)^2 \le \omega^2$; $-i\sqrt{(\epsilon_{n\mu}\beta)^2-\omega^2}$ if $(\epsilon_{n\mu}\beta)^2 > \omega^2$
$\gamma(r)$ = local lean angle (Fig. 2)
$\epsilon_{n\mu}$ = modal eigenvalue
η = transformed chordwise coordinate
θ = angular coordinate
Λ = number of chordwise loading functions
λ = tip lean angle, summation integer
μ = radial mode index
ξ = axial source coordinate
ρ = radial source coordinate, mass density
τ = source time coordinate
φ = angular source coordinate
$\varphi_j(\rho)$ = angular coordinate of jth vane
ψ = wake fixed angular coordinate
Ω_w = angular velocity of wake system
ω = radian frequency (i.e., Fourier transform variable)

Superscripts

$(\tilde{\ })$ = in time domain
$(\bar{\ })$ = pure tone
$(\ )^+$ = axially positive of source
$(\ )^-$ = axially negative of source

Subscripts

f = point force
L = leading edge
n = normal
r = radial
T = trailing edge
w = wake
x = axial
θ = tangential

Presented as Paper 81-0091 at the AIAA 19th Aerospace Sciences Meeting, St. Louis, Mo., Jan. 12-15, 1981; submitted March 11, 1981; revision received Feb. 22, 1982.

*Research Engineer, Dept. of Fluid Dynamics. Member AIAA.

Introduction

FOR current high-bypass jet engines the fan noise level in the approach phase of the flight often proves to be the most critical component of total aircraft noise. The origin of this type of noise is the interaction of velocity disturbances

and fan rotor blades or stator vanes. These disturbances may consist of ingested atmospheric turbulence, asymmetric inflow, boundary-layer turbulence, or wakes shed from an upstream row of blades. Also a secondary flowfield caused by viscous-inviscid interaction between wall boundary layers and blade pressures can bring about noise when impinging on a downstream blade row.

The need for prediction methods of fan noise extends beyond overall quantities such as the acoustic power. Since the performance of an acoustic liner depends largely on the detailed composition of the sound field, the modal distribution of the sound generated must also be known.

In the past, lifting line (compact source) approximations of the blades have been widely used in prediction techniques, e.g., see Refs. 1 and 2. Obviously, such approximations neglect any interference of the chordwise-distributed unsteady pressure. A more advanced method based on a lifting surface approach for two-dimensional cascades of blades was presented in 1970 by Kaji and Okazaki.[3] As shown explicitly by Kaji[4] the compact source approximation fails when the sound wave length is not large compared with the blade chord, as is usually the case in turbomachinery.

Although a two-dimensional cascade is a reasonable approximation for a blade row in a thin annular duct, the current low hub/tip ratio fans are not very well modeled by a two-dimensional representation. A three-dimensional lifting surface theory for the sound generated by a blade row in a uniform subsonic flow was presented in 1977 by Namba.[5] He analyzed the aerodynamic and acoustic response of a lightly loaded fan rotor to small harmonic flow distortions. The blades in his theory have a constant axial extent, without sweep or lean. These restrictions on the blade geometry limit the usefulness of his theory since planform variation and vane lean can be employed to influence the sound characteristics of a blade row. In particular, stators (which are less subject to structural constraints than rotors) may be suited to this method of noise control. The effect of leaned outlet guide vanes exposed to a rotor wake system is intriguing since considerable noise reduction was experimentally found by Nemec[6] in the reverse case of leaned wakes impinging on a rotor. The usual explanation of this reduction is that wake lean will result in a spanwise phasing of the unsteady lift response and so excite the higher radial duct modes at the cost of the lower ones. The higher radial duct modes carry less energy for a given magnitude than the lower ones and beyond the cut-off limit the transport of acoustic energy into an anechoic duct ceases completely. The argument, however, also applies to leaned outlet guide vanes in a rotor wake system and the idea that lean in at least one direction must be beneficial seems to have been widely accepted.[7-10]

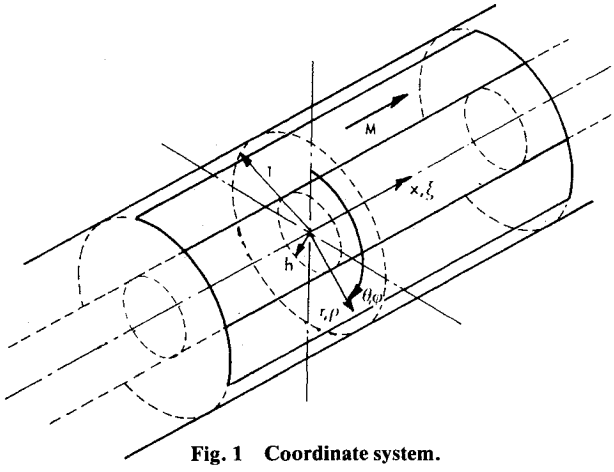

Fig. 1 Coordinate system.

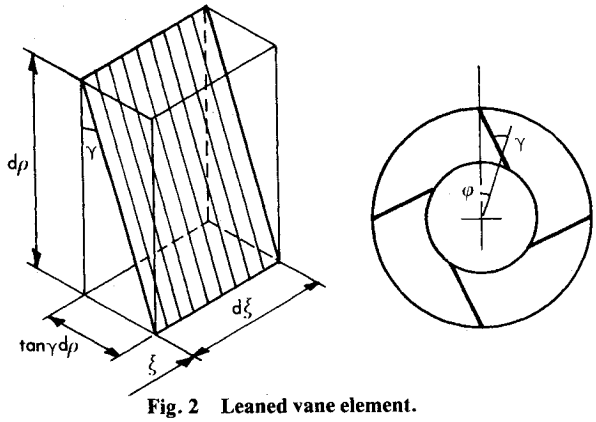

Fig. 2 Leaned vane element.

The present paper will show that theoretically, in most conditions, the application of vane lean in a typical stator raises the noise level considerably.

The present theory extends Namba's analysis[5] to include vane lean and explicitly includes nonharmonic velocity disturbances such as turbulence. Furthermore, the analysis of the problem deviates in a few points from Namba's approach. Since for structural reasons lean can be applied only to stator vanes, the simplifications that can be made for a stator will be exploited.

Analysis

An anechoic hard-walled annular duct carrying a uniform inviscid main flow of subsonic Mach number M is considered. Taking the duct outer radius, the main flow mass density, and sound speed as scaling parameters, a *nondimensional formulation* will be used throughout. Then, the governing linearized equations for small perturbations of the main flow read† in duct-fixed coordinates

$$\frac{\partial\tilde{\rho}}{\partial t}+M\frac{\partial\tilde{\rho}}{\partial x}+\nabla\cdot\tilde{v}=0 \tag{1}$$

$$\frac{\partial\tilde{v}}{\partial t}+M\frac{\partial\tilde{v}}{\partial x}+\nabla\tilde{p}=\tilde{F} \tag{2}$$

$$\tilde{p}=\tilde{\rho} \tag{3}$$

Here the x axis has been chosen along the duct axis (Fig. 1). The external force field $\tilde{F}$ will be identified later with the pressure jump distribution across the stator vanes in the duct. These vanes are modeled as unstaggered and uncambered rigid surfaces of negligible thickness and constant chord. For brevity the word "perturbation" will be omitted in the following. The hard-wall boundary condition requires the radial velocity to vanish at hub ($r=h$) and casing ($r=1$). Velocity and mass density can be eliminated from the above equations to obtain the convected-wave equation

$$\left(\nabla^2-\frac{\partial^2}{\partial t^2}-2M\frac{\partial^2}{\partial x\partial t}-M^2\frac{\partial^2}{\partial x^2}\right)\tilde{p}=\nabla\cdot\tilde{F} \tag{4}$$

The standard way to solve this equation is to construct first the Green's function $\tilde{G}$, which may be regarded as the field of an impulsive, omnidirectional point source or monopole, and to find subsequently $\tilde{p}$ as a function of $\tilde{F}$ by integration.

The equation for $\tilde{G}$ is

$$\left(\nabla^2-\frac{\partial^2}{\partial t^2}-2M\frac{\partial^2}{\partial x\partial t}-M^2\frac{\partial^2}{\partial x^2}\right)\tilde{G}$$

$$=-\delta(x-\xi)\delta(r-\rho)\frac{\delta(\theta-\varphi)}{\rho}\delta(t-\tau) \tag{5}$$

†Quantities marked with a tilde (~) are given as a function of time. When Fourier transformed in time the tilde is omitted.

where x, r, and θ are cylindrical field coordinates (Fig. 1) and ξ, ρ, and φ the corresponding source coordinates. The source time coordinate is denoted by τ. The Green's function is conventionally found as a Fourier-Bessel series in the space coordinates and a Fourier integral in time.[5,11]

By differentiating Eq. (5) with respect to the source coordinates, it is easily shown that the pressure field p_f of an impulsive point force (f_x,f_r,f_θ) acting in (ξ,ρ,φ,τ) is given by

$$p_f = f_x \frac{\partial G}{\partial \xi} + f_r \frac{\partial G}{\partial \rho} + \frac{1}{\rho} f_\theta \frac{\partial G}{\partial \varphi} \tag{6}$$

Next, the impulsive point force is identified with the force exerted by a small surface element of the jth vane in a stator during time $d\tau$. If the pressure difference across the jth vane is denoted by $\Delta\tilde{p}_j(\xi,\rho,\tau)$ we have (Fig. 2)

$$\begin{aligned} f_x &= 0 \\ f_r &= \tan\gamma(\rho)\,\Delta\tilde{p}_j\,d\xi\,d\rho\,d\tau \\ f_\theta &= \Delta\tilde{p}_j\,d\xi\,d\rho\,d\tau \end{aligned} \tag{7}$$

In Namba's analysis[5] $\gamma(\rho)$ is zero everywhere and as a result radial forces are absent. As is usual in practice, only stators with identical and equally spaced vanes are considered and the angular coordinate $\varphi_j(\rho)$ of the jth vane is given by

$$\varphi_j(\rho) = \varphi_0(\rho) + j(2\pi/N) \tag{8}$$

where N is the number of vanes in the stator. Substitution of Eqs. (7) and (8) into Eq. (6) followed by integration over the vane surfaces and the source time τ (of which the latter is recognized as the Fourier transform of $\Delta\tilde{p}_j$) leads to the following expression for the pressure field of a complete stator with leaned vanes

$$\begin{aligned} p = \frac{-1}{4\pi} \sum_{n=-\infty}^{\infty} \exp(in\theta) \sum_{\mu=1}^{\infty} U_{n\mu}(r) \int_h^1 \int_{x_L}^{x_T} \exp[-in\varphi_0(\rho)] \\ \times \frac{U_{n\mu}(\rho)}{\beta_{n\mu}} f_{n\mu}(\rho) \exp\left\{ \frac{i(x-\xi)}{\beta^2} [\omega M - \mathrm{sgn}(x-\xi)\beta_{n\mu}] \right\} \\ \times \sum_{j=0}^{N-1} \exp\left(-inj\frac{2\pi}{N}\right) \Delta p_j(\xi,\rho,\omega)\,d\xi\,d\rho \end{aligned} \tag{9}$$

from which the modal amplitudes $A_{n\mu}$ can be readily identified as surface integrals over the vanes.

Equation (9) is an important result since it states explicitly how the pressure field depends on the pressure jump distribution over the vanes. However, this distribution is usually unknown. It will be determined by applying the boundary condition not used until now, viz., that of vanishing normal velocity at the vane surfaces. This normal velocity results from external velocity disturbances and the velocity induced by the vanes. First, the induced velocity will be derived. Upon taking Fourier transforms in t and x of the linearized momentum equation (2) the causal solution of the induced velocity is found to be $(M>0)$

$$v = \frac{1}{M} \exp\left(-\frac{i\omega x}{M}\right) \int_{-\infty}^{x} \exp\left(\frac{i\omega x'}{M}\right) (F - \nabla p)\,dx' \tag{10}$$

Obviously, the velocity depends on both force and pressure terms. At this point, the present analysis essentially deviates from Namba's approach,[5] in which the blade surfaces are unnecessarily excluded from the domain of the solution and force terms do not explicitly occur. As a result the normal velocity becomes singular at the blade surfaces. Then a laborious and delicate process of separating the singular parts from the solution is necessary to produce the correct solution. In the present analysis the solution of the normal velocity has a *regular behavior at the vane surfaces* since the pressure discontinuity is just balanced by the vane force "sheets." The external force field $\tilde{F}$ written as a function of the pressure difference across the vanes reads

$$\begin{aligned} \tilde{F} = \int_{-\infty}^{\infty} \int_h^1 \int_{x_L}^{x_T} \delta(t-\tau)\delta(x-\xi) \frac{\delta(r-\rho)}{\rho} [\tan\gamma(\rho)\,\boldsymbol{i}_r + \boldsymbol{i}_\theta] \\ \times \sum_{j=0}^{N-1} \delta\left[\theta - \varphi_0(\rho) - j\frac{2\pi}{N}\right] \Delta p_j(\xi,\rho,\tau)\,d\xi\,d\rho\,d\tau \end{aligned} \tag{11}$$

Using the cross-sectional eigenfunctions to expand the delta functions in r and θ and taking the Fourier transform in time, the resulting force field $\boldsymbol{F}$ is substituted in Eq. (10). Then the normal velocity v_n is given by[11]

$$\begin{aligned} v_n = \frac{1}{2\pi M} \sum_{n=-\infty}^{\infty} \exp(in\theta) \sum_{\mu=1}^{\infty} U_{n\mu}(r) \int_h^1 \int_{x_L}^{x_T} \exp[-in\varphi_0(\rho)] \\ \times FD_{n\mu}(x,r,\xi,\rho,\omega) \sum_{j=0}^{N-1} \exp\left(-inj\frac{2\pi}{N}\right) \Delta p_j(\xi,\rho,\omega)\,d\xi\,d\rho \end{aligned} \tag{12}$$

In the function $FD_{n\mu}$ (see Appendix A) the irrotational acoustic velocity field and a vorticity field can be distinguished. The acoustic velocity is marked by the individual axial dependence of every mode (i.e., n, μ combination). Furthermore, the acoustic field is present on both sides of the source region. On the other hand, the vorticity field extends only downstream of a vane element, which is expressed by the Heaviside function $H(x-\xi)$. The axial periodicity of the vorticity does not depend on the mode but is entirely fixed by the Strouhal number ω/M.

Now for an external velocity disturbance field with normal component $w_n(x,r,\theta,\omega)$ the condition of flow tangency on the vanes produces the following set of N integral equations (for N vanes)

$$\left[v_n(x,r,\theta,\omega) + w_n(x,r,\theta,\omega) = 0 \right]_{\theta=\varphi_0(r)+\ell(2\pi/N)}^{x_L<x<x_T \quad h<r<1} \tag{13}$$

where ℓ $(=0,1,\ldots N-1)$ indicates the vane to which the condition is applied. In practice, N is usually a large number. Fortunately, it is possible to reduce the number of equations involved. To this end the external field w_n is expanded into a circumferential Fourier series as follows

$$w_n(x,r,\theta,\omega) = \sum_{k=-\infty}^{\infty} w_k(x,r,\omega)\exp(ik\theta) \tag{14}$$

Further, let $\Delta p_{kj}(\xi,\rho,\omega)$ be the pressure jump across the jth vane caused by the kth term in Eq. (14). Then it is easily seen that the $(j+1)$th vane will experience an identical velocity disturbance with a phase shift $k(2\pi/N)$. Thus Δp_{kj} can be expressed in the pressure jump across the zeroth vane $\Delta p_{k,0}$ as

$$\Delta p_{kj} = \exp\left(ikj\frac{2\pi}{N}\right) \Delta p_{k,0} \tag{15}$$

Now the summation over j (the vanes), as occurs in the expressions for pressure [Eq. (9)] and induced normal velocity [Eq. (12)], greatly reduces since

$$\begin{aligned} \sum_{j=0}^{N-1} \exp\left(-imj\frac{2\pi}{N}\right) \Delta p_{kj} &= N\Delta p_{k,0} \quad \text{if } m = k - nN \\ &= 0 \quad \text{if } m \neq k - nN \end{aligned} \tag{16}$$

for any integer n. Moreover all of Eqs. (13) become identical and only one equation has to be solved. The price to be paid

for this saving is the repeated evaluation of the integral equation for every k component in the expansion of the velocity disturbance field. The remaining equation to be solved is as follows

$$\left[\frac{N}{2\pi M}\sum_{n=-\infty}^{\infty}\exp[im\varphi_0(r)]\sum_{\mu=1}^{\infty}U_{m\mu}(r)\right.$$

$$\times\int_h^1\int_{x_L}^{x_T}\exp[-im\varphi_0(\rho)]FD_{m\mu}(x,r,\xi,\rho,\omega)\Delta p_{k,0}(\xi,\rho,\omega)\,d\xi\,d\rho$$

$$\left.=-w_k(x,r,\omega)\exp[ik\varphi_0(r)]\right]_{h<r<1}^{x_L<x<x_T} \tag{17}$$

Solution Procedure

The first step to solve the integral equation (17) is the expansion of the unknown distribution $\Delta p_{k,0}$ in a chordwise and spanwise Fourier series. However, since the analysis is for inviscid flow, the solution of Eq. (17) is not unique. The amount of vorticity shed from the trailing edge has to be fixed in some way. In the present case, the full Kutta condition is adopted, i.e., the fluid particles are assumed to leave the trailing edge tangentially. This condition is equivalent to the requirement of no singular behavior of the pressure jump across the vanes at the trailing edge. At the leading edge, of course, a singularity is to be expected. In subsonic flow the possible edge singularities in the pressure jump are of the $1/\sqrt{x}$ type. To identify such singularities in the Fourier series is difficult. Therefore, Glauert's transformation[12] is applied to the axial coordinate ξ as follows

$$\frac{\xi-x_L}{x_T-x_L}=\frac{1-\cos\eta}{2},\qquad 0<\eta<\pi \tag{18}$$

The essential point in this Glauert transformation is that integrable $1/\sqrt{x}$ edge singularities are transformed into nonintegrable $1/\eta$ singularities. These $1/\eta$ singularities correspond to divergent Fourier series in η, implying that a convergent series relates to a distribution free of singularities. Hence, the complete solution satisfying the Kutta condition can be written as a convergent Fourier expansion in η, completed by a leading-edge singularity term (i.e., a Glauert series). In two-dimensional steady incompressible thin-airfoil theory the Fourier coefficients of this expansion and the magnitude of the singularity can be explicitly determined.[12] Unfortunately, such a direct solution procedure seems to be impossible for the present three-dimensional unsteady compressible flow problem.

However, if the Glauert series is adopted to describe the chordwise pressure jump distribution, the convergence of the Fourier expansion can be estimated from the numerically found (see below) Fourier coefficients. If the decay of these coefficients indicates a convergent Fourier expansion a strong, a posteriori, argument that the solution satisfies the Kutta condition is obtained. As a result, the pressure jump distribution is written as

$$\Delta p_{k,0}=\sum_{j=1}^{\infty}\cos\left\{(j-1)\left(\frac{\rho-h}{1-h}\right)\pi\right\}\left[P_{kj1}(\omega)\cot\left(\frac{\eta}{2}\right)\right.$$

$$\left.+\sum_{\lambda=2}^{\infty}P_{kj\lambda}(\omega)\sin\{(\lambda-1)\eta\}\right] \tag{19}$$

where the expression in square brackets is the classical Glauert series. As opposed to what is frequently claimed, although not in Ref. 12, the choice of sine functions in the η expansion is irrelevant with respect to the Kutta condition. The reason to take this half-range trigonometric series is a faster and uniform convergence.

Table 1 Rotor and stator data, standard case

Number of rotor blades, V	19
Number of stator vanes, N	20
Hub/tip ratio, h	0.4
Rotor axial chord length	0.1
Stator chord	0.1
Rotor-stator spacing	0.2
Axial Mach number, M	0.3
Rotor circumferential tip Mach number, Ω_w	0.7
Rotor blade drag coefficient, c_d	0.02
Wake lean angle	0.0

Table 2 Computational data, standard case

Wake component index, k	19
Modal index, m $(=k-nN)$	$n(-10,-9,\ldots,10)$
Modal index, μ	$\mu(1,2,\ldots 11)$
Chordwise expansion, $\Delta p_{k,0}$	$\Lambda=6$
Spanwise expansion, $\Delta p_{k,0}$	$J=6$
Collocation scheme	6×6
No. of axial integration steps	48
No. of radial integration steps	48

Substitution of the series of Eq. (19) into Eq. (17) gives an identity in (x,r), determining the coefficients $P_{jk\lambda}$. Restricting this identity to $J\times\Lambda$ collocation points and a corresponding truncation of the series yield a system of linear algebraic equations for approximations of $P_{kj\lambda}$ $(j=1,2,\ldots J,$ $\lambda=1,2,\ldots\Lambda)$. Upon making the series in n and μ of Eq. (17) finite, the matrix elements of the system are computed. The required high-order radial eigenfunctions are obtained by means of Namba's method.[13] The chordwise and spanwise integrations are performed numerically. The collocation points are uniformly distributed in both η and r directions. Finally, the system is solved by means of standard matrix techniques. A computer program based on this solution procedure takes about 250 CPU seconds on a CDC Cyber 73 system for a typical case.

Acoustic Effect of Vane Lean

To investigate the effect of vane lean, calculations of the sound field of a typical stator exposed to the periodic wake system of an upstream rotor were made. The stator has leaned flat vanes. Relevant data on the standard configuration of the rotor-stator assembly are given in Table 1. A simple wake diffusion model (see Appendix B) has been used to synthesize the velocity disturbance field caused by the rotor blades. These blades are considered to be acoustically transparent generators of viscous wakes only. The velocity disturbance field is controlled by the drag coefficient of the blades which is generally a function of the radius. As indicated in Table 1, a constant drag coefficient is employed in the standard case. The 19 lobe rotor wake system produces a pure-tone Tyler-Sofrin[14] interaction with the 20 stator vanes at the fundamental blade passing frequency ($19\Omega_w=13.3$) and higher harmonics. The present numerical evaluation will be restricted to the fundamental blade passing frequency. Then three modes of circumferential mode index $m=1$ are cut-on. In this pure-tone example (see also Appendix B), the pressure coefficients can be written as

$$P_{19,j\lambda}(\omega)=\bar{P}_{19,j\lambda}\delta(\omega+19\Omega_w) \tag{20}$$

The pressure jump distribution and the modal amplitudes are written similarly. As a characteristic measure of the sound field the (upstream and downstream) acoustic power generated by the source is a most suitable quantity. Following Morfey[15] and ignoring the rotor wakes and trailing vortices, the pure-tone modal power $W_{m\mu}$ emitted outward from the

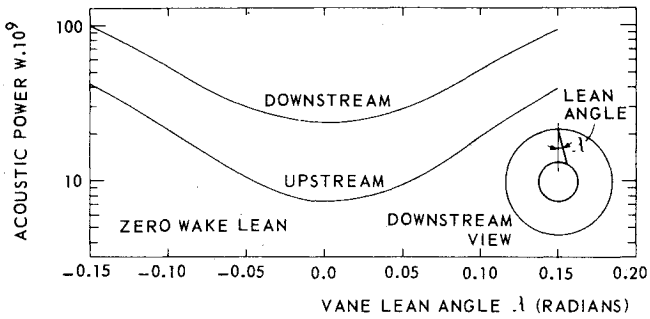

Fig. 3 Effect of vane lean angle, conditions in Table 1.

source is written as

$$W^{\pm}_{m\mu} = \frac{\beta^2 \beta_{m\mu} |\bar{A}^{\pm}_{m\mu}|^2}{\pi\omega_k \left(1 \mp \frac{M\beta_{m\mu}}{\omega_k}\right)^2} \quad \text{if } \beta_{m\mu} \text{ is real (cut-on)}$$

$$= 0 \quad \text{if } \beta_{m\mu} \text{ is imaginary (cut-off)} \qquad (21)$$

where, in the present example, $\omega_k = -k\Omega_w$. Per frequency, the total power is the sum of the modal powers. In Eq. (21) the return to the physical time domain has been accounted for and either positive or negative k values only should be taken.

It is noted that the power has been made dimensionless on (mean density) × (sound speed)^3 × (outer duct radius)^2. The standard number of terms in each of the series occurring in the analysis is listed in Table 2. In the present example these numbers proved to be amply sufficient for a well-converged acoustic power. Detailed information on the convergence of the solution is given in Ref. 11. The decay of the pressure coefficients appeared to be fast enough to provide a strong argument that the Kutta condition was indeed satisfied.

It is easily grasped that the application of vane lean in a stator, on which an orderly structured wake system impinges, will affect the production of sound. If the wakes are radially oriented, vane lean introduces a spanwise phasing of the aerodynamic response of the vanes. As a result the higher radial modes will be excited predominantly and the modal distribution of the sound field drastically changes. As pointed out in the introduction, the idea that vane lean must be beneficial in at least one direction is widely accepted. However, as shown in Fig. 3 the present theory predicts a distinct adverse effect of lean on the noise level in the standard case (Tables 1 and 2). To trace the origin of this effect, the behavior of the amplitudes of the cut-on modes is investigated. In the present case three modes are cut-on at the blade passing frequency. As Fig. 4 shows, there is a strong tendency toward the higher radial modes when lean is applied. However, this growth is much more rapid than the decrease of the lowest (1,1) modal amplitude and the net effect is a sharp increase in total power. To understand this phenomenon it must be realized that, apart from a spanwise phasing of the lift response, lean also implies a radially nonuniform vane displacement, an enlargement of the vane surfaces, and a radial component of the vane forces.

In the present case, the vane displacement is small compared to 2π, the circumferential period of the cut-on modes ($m = 1$), and is not likely to be responsible for such large effects. Also the vane surface enlargement is too small to explain this increase of power. Apparently the radial component of the vane forces causes the sound increase. Thus, the situation is entirely different from the case where leaned wakes impinge on radial stator vanes, as is confirmed in Fig. 5. Here, wake lean has hardly any effect on the emitted sound power. The modal breakdown given in Fig. 6 shows that in this case the increase of the higher radial modes is ap-

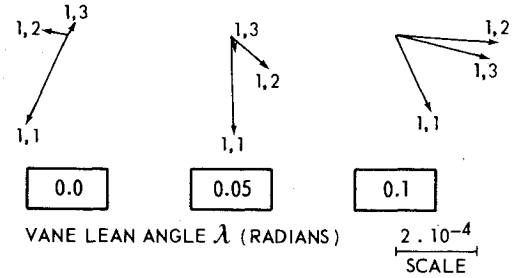

Fig. 4 Effect of vane lean angle, complex plane representation of modal amplitudes (m,μ) at upstream station $(x = x_L - 0.4$ for each triad of vectors the origin at the center, conditions in Table 1.

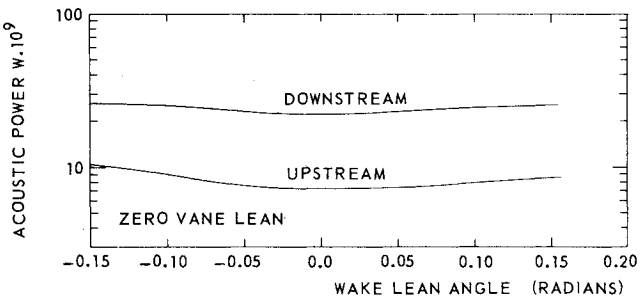

Fig. 5 Effect of wake lean angle, conditions in Table 1.

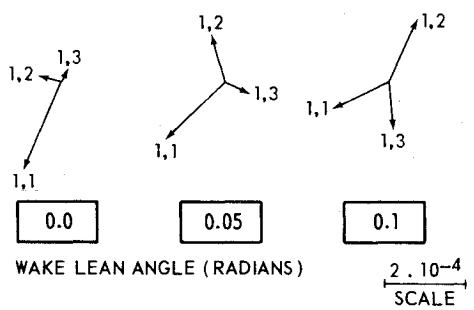

Fig. 6 Effect of wake lean angle, complex plane representation of modal amplitudes (m,μ) at upstream station $x = x_L - 0.4$ for each triad of vectors the origin at the center, conditions in Table 1.

proximately compensated by the decrease of the lowest (1,1) radial mode. The intriguing question: "What happens when wake and vane lean are combined?" is answered in Fig. 7. Here the results show that at a given wake lean of 0.1 rad the minimum noise vane lean angle has undergone only a marginal shift from the case of radial wakes (Fig. 3). The power level at 0.1 vane lean, where the spanwise phasing of the disturbance velocity is minimal, is significantly higher than at zero lean. So, even in this case, a radial vane alignment seems to be the best choice for a low noise level.

A satisfactory physical explanation of this lean effect is not easily given. In the analysis, however, we can indicate a powerful term which vanishes at zero vane lean. This term is the first one of the function $f_{m\mu}(\rho)$ [Eq. (A2)] which occurs both in the governing integral equation (17) and in the modal pressure amplitudes given by Eq. (9). The first term in $f_{m\mu}(\rho)$ determines the contribution of the radial component of the local vane force to the modal field and appears only when lean is applied. Due to the presence of $U'_{m\mu}(\rho)$ it can easily become larger than the second term, which determines the circumferential contribution, provided m is a small number as in the present example ($m = 1$). The computed pressure jump distributions $\overline{\Delta p}$ show different shapes for cases with vane lean and the corresponding wake lean at zero vane lean. In particular the imaginary part of $\overline{\Delta p}$ exhibits more radial

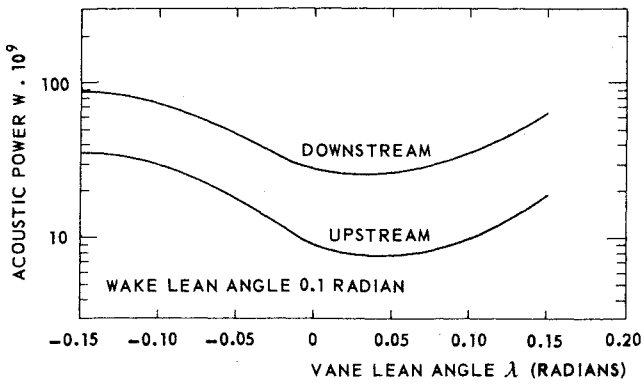

Fig. 7 Effect of vane lean for a leaned wake system, conditions in Table 1.

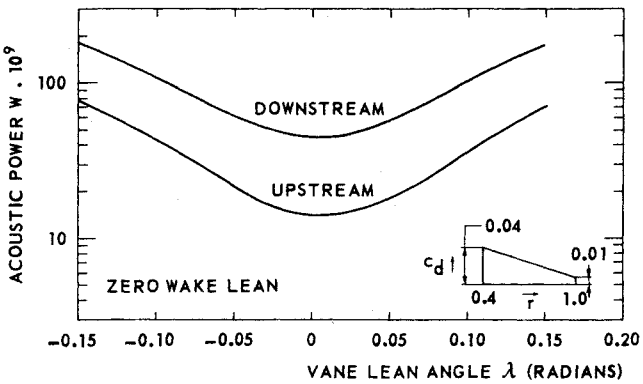

Fig. 8 Acoustic power for a linear distribution of the rotor blade drag coefficient, conditions in Table 1.

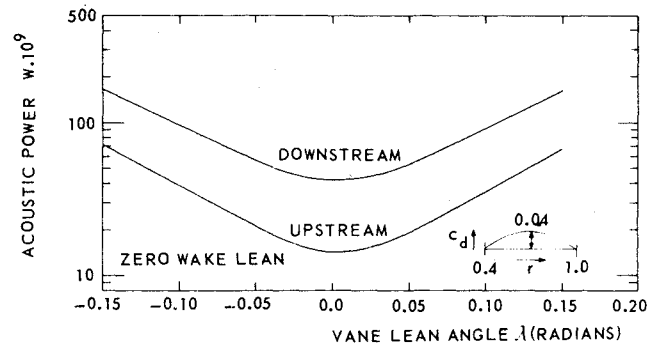

Fig. 9 Acoustic power for a parabolic distribution of the rotor blade drag coefficient, conditions in Table 1.

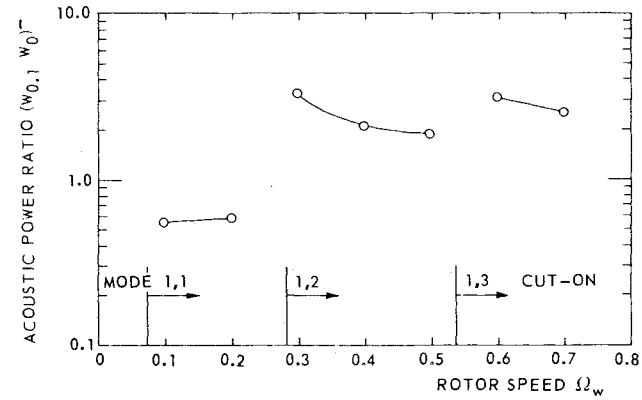

Fig. 10 Ratio of upstream powers for 0.1 and zero vane lean at different rotor speeds, conditions in Table 1.

waviness in the case of vane lean. The overall level of $\overline{\Delta p}$, however, is the same in both cases. Apparently, the local behavior of $f_{m\mu}(\rho)$ and details of $\overline{\Delta p}$ are responsible for the acoustic effect of vane lean. Since the extremes of $U'_{m\mu}(\rho)$ are approximately proportional to the radial mode order μ, it fits our observations that the modal amplitudes of the higher μ modes are mostly affected by lean.

The above results are calculated for a single distribution of the rotor blade drag coefficient, viz., a constant 0.02 value. The effect of this constant value is that the disturbance level is highest in the tip region. To examine the effect of different disturbance velocity fields, the radial distribution of the rotor blade drag coefficient was varied. In Fig. 8 a linear variation of the drag coefficient from 0.04 at the hub to 0.01 at the tip has been applied. Obviously, this variation enhances the disturbance velocity in the hub region. The response to lean does, however, not deviate significantly from the standard case with a constant drag coefficient (Fig. 3). Virtually the same behavior is observed in Fig. 9 where a parabolic variation of the rotor blade drag coefficient has been used. So, in the present example, the acoustic power response to vane lean proves to be practically independent of the radial shape of the disturbance velocity field.

Finally the question arises whether there exists any frequency range where vane lean is beneficial. Since a slight decrease of the (1,1) modal amplitude can be observed when lean is applied there could be a power decrease if the (1,1) mode is the only cut-on mode. Therefore the ratio of the sound power for 0.1 vane lean and zero lean is presented for different rotor speeds in Fig. 10. When the rotor speed is between 0.08 and 0.28, only the (1,1) mode is cut-on and then lean actually gives a sound reduction. However, once the second mode becomes cut-on the ratio jumps to a value well above 1 and the advantage of lean is nullified. So low-speed fans may occasionally benefit by vane lean but this is not very likely to happen in an aeroengine fan stage. No attempt was made to follow the behavior of the power ratio through the cut-on frequencies since the integral equation (17) is singular there ($\beta_{m\mu} \to 0$) and probably demands a local analysis.

Conclusions

An unsteady three-dimensional lifting surface theory to predict the sound field of a stator with nonradial vanes has been developed in the present paper. With respect to the earlier theory of Namba,[5] the introduction of vane lean is the new element. By taking into account both force and pressure terms in the momentum equation the analysis progresses more smoothly than in Ref. 5. The essential role of the Glauert transformation with respect to the singularities has been elucidated.

The effect of vane lean has been investigated numerically by means of a typical example of a stator exposed to the viscous wake system of a rotor. The modal distribution, as well as the total power of the sound field, proves to be very sensitive to lean variation. As opposed to a widely accepted opinion, a progressive power increase results when vane lean is applied. Surprisingly, this behavior is similar for both positive and negative lean. No influence of the radial distribution of velocity disturbances on the power response to lean is found. The essential impact of vane lean on sound generation is emphasized by comparison with the sound field of radial vanes exposed to leaned wakes, giving the same incident velocity field at a vane. In that case the sound power is practically invariant with respect to the wake lean angle (although the modal distribution varies considerably). These different acoustic effects of wake and vane lean can be associated with the appearance of a radial component in the force distribution of a leaned vane stator.

Still, there is a frequency range where vane lean is beneficial. This is the case where only one mode is cut-on. However, such a condition is unlikely to occur in a turbofan engine.

Appendix A: Auxiliary Functions

$$FD_{m\mu}(x,r,\xi,\rho,\omega) = U_{m\mu}(\rho)\,V_{m\mu}(r,\rho,\omega)\exp\left[-\frac{i\omega}{M}(x-\xi)\right]$$

$$\times H(x-\xi) + \frac{\beta^2 U_{m\mu}(\rho)}{2\beta_{m\mu}} f_{m\mu}(\rho)\,g_{m\mu}(r)\left(\exp\left\{\frac{i(x-\xi)}{\beta^2}\left[\omega M - \operatorname{sgn}(x-\xi)\beta_{m\mu}\right]\right\}\Big/\left[\operatorname{sgn}(x-\xi)\beta_{m\mu} - \frac{\omega}{M}\right]\right) \tag{A1}$$

$$f_{m\mu}(\rho) = i\frac{U'_{m\mu}(\rho)}{U_{m\mu}(\rho)}\tan\gamma(\rho) + \frac{m}{\rho} \tag{A2}$$

$$g_{m\mu}(r) = i\frac{U'_{m\mu}(r)}{U_{m\mu}(r)}\sin\gamma(r) - \frac{m}{r}\cos\gamma(r) \tag{A3}$$

$$h_{m\mu}(\rho,\omega) = \frac{\beta^2 M^2 f_{m\mu}(\rho)}{\omega^2 - M^2\beta^2_{m\mu}} \tag{A4}$$

$$V_{m\mu}(r,\rho,\omega) = \tan\gamma(\rho)\sin\gamma(r) + \cos\gamma(r) + h_{m\mu}(\rho,\omega)\,g_{m\mu}(r) \tag{A5}$$

Appendix B: Blade Wakes as Velocity Disturbances

The velocity disturbances of a viscous rotor wake system at a given radius are calculated as if they were generated by a two-dimensional cascade of blades, so the disturbance velocity has a zero radial component.

A rectangular coordinate system s, q is taken (see Fig. B1) with its origin at the trailing edge of the zeroth rotor blade. The positive s axis is in the direction of the relative flow. The local chord of the rotor blade is denoted by c. The wake is characterized by its width Y and the wake center velocity w_c. The undisturbed velocity is symbolized by w_e. Now the wake diffusion is modeled as

$$w_e - w_c = w_e\sqrt{c_d c/s} \qquad Y = \sqrt{c_d sc} \tag{B1}$$

where c_d is the local blade drag coefficient. Further, a cosine wake profile is assumed. In the present case, the undisturbed velocity is given by

$$w_e = \sqrt{(\Omega_w r)^2 + M^2} \tag{B2}$$

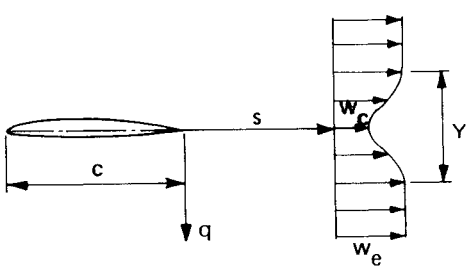

Fig. B1 Rotor blade wake model nomenclature.

Now the wake velocity is transformed to an x, ψ system where ψ is an angular coordinate fixed to the rotor. In this system the following Fourier expansion of V identical and equally spaced wakes is made

$$w(x,r,\psi) = \sum_{k=-\infty}^{\infty} w_k(x,r)\exp(ikV\psi) \tag{B3}$$

where the Fourier coefficients $w_k(x,r)$ are evaluated numerically. Finally, transformation to the duct-fixed system via $\psi = \theta - \Omega_w t$ and taking the normal component of the velocity at the vanes yields $\tilde{w}_n(x,r,\theta,t)$.

Acknowledgments

The present investigation was sponsored by the Netherlands Agency for Aerospace Programs (NIVR). The author is indebted to Prof. P. J. Zandbergen and Dr. S. W. Rienstra for many helpful discussions and valuable comments. In particular, they contributed to the understanding of the role of the Glauert transformation in relation to the solution satisfying the Kutta condition. The numerics involved were carefully analyzed by Mr. W. Vaatstra.

References

[1] Benzakein, M. J., "A Study of Fan-Compressor Noise Generation," *Basic Aerodynamic Noise Research*, NASA SP-207, 1969, pp. 257-274.

[2] Dittmar, J. H., "Methods for Reducing Blade Passing Frequency Noise Generated by Rotor-Wake Stator Interaction," NASA TM X-2669, Nov. 1972.

[3] Kaji, S. and Okazaki, T., "Generation of Sound by Rotor-Stator Interaction," *Journal of Sound and Vibration*, Vol. 13, No. 3, 1970, pp. 281-307.

[4] Kaji, S., "Noncompact Source Effect on the Prediction of Tone Noise from a Fan Rotor," AIAA Paper 75-446, March 1975.

[5] Namba, M., "Three-Dimensional Analysis of Blade Force and Sound Generation for an Annular Cascade in Distorted Flows," *Journal of Sound and Vibration*, Vol. 50, No. 4, 1977, pp. 479-508.

[6] Nemec, J., "Noise of Axial Fans and Compressors: Study of Its Radiation and Reduction," *Journal of Sound and Vibration*, Vol. 6, No. 2, 1967, pp. 230-236.

[7] Benzakein, M. J., "Research on Fan Noise Generation," *Journal of the Acoustical Society of America*, Vol. 51, No. 5, Pt. 1, 1972, pp. 1427-1438.

[8] Kazin, S. B., "Radially Leaned Outlet Guide Vanes for Fan Source Noise Reduction," NASA CR-134486, Nov. 1973.

[9] Cornell, W. G., "Experimental Quiet Engine Program—Summary Report," NASA CR-2519, March 1975.

[10] Schloemer, J. J. and Tabakoff, W., "Technique for Calculating the Pure Tone Acoustic Power of a Turbomachinery Stage," AIAA Paper 79-0184, Jan. 1979.

[11] Schulten, J.B.H.M., "A Lifting Surface Theory for the Sound Generated by the Interaction of Velocity Disturbance with a Leaned Vane Stator," AIAA Paper 81-0091, Jan. 1981 (also NLR MP 80041 U).

[12] Glauert, H., *The Elements of Aerofoil and Airscrew Theory*, 2nd Ed., Cambridge University Press, England, 1959.

[13] Namba, M., "Lifting Surface Theory for a Rotating Subsonic or Transonic Blade Row," British R&M 3740, Nov. 1972.

[14] Tyler, J. M. and Sofrin, T. G., "Axial Flow Compressor Noise Studies," *SAE Transactions*, Vol. 70, 1962, pp. 309-332.

[15] Morfey, C. L., "Sound Generation in Ducts with Flow," *Journal of Sound and Vibration*, Vol. 14, No. 1, 1971, pp. 37-55.